Mathematical modeling of the electrochemical behavior of a polyaniline film for the fast electron transfer kinetic

Fatemeh Ziaei Moghaddam, Reza Arefinia *

Chemical Engineering Department, Faculty of Engineering, Ferdowsi University of Mashhad, Mashhad, Iran

ABSTRACT

The electrochemical behavior of a polyaniline (PANI) film as a conductive polymer has been studied using a new proposed mathematical model (PMM). A one-dimensional transient model, considering the doping-dedoping and redox processes for a thin PANI film, was developed based on the cyclic voltammetry method. It was assumed that two reactions occur at the interface of film/electrolyte during the potential sweep: an electrochemical reaction and an adsorption-desorption reaction. The diffusion process of dopant ions was governed by Fick's second law equation. The modeling results were evaluated using the experimental data reported in the literature. The effect of different parameters including bulk concentration of dopants (C_A^*), potential scan rate (v), adsorption rate constant (k_{ad}) and desorption rate constant (k_{de}), on the electrochemical behavior of a PANI film were parametrically studied using the PMM. The increase of k_{ad} and C_A^* causes the shift of redox couple to the lower potentials while the increment of k_{de} moves the redox couple to the higher potentials. The increase of parameter v was provides the enhancement of both peak couple currents and the higher peak potential separation.

© 2018 Elsevier B.V. All rights reserved.

1. Introduction

Conductive polymers (CPs) have been received extensive attention since discovering their electrical and electrochemical properties [1–4]. Among various CPs, polyaniline (PANI) has more promising advantages in different applications such as anti-corrosion coatings [5,6], sensors [7–9], electrochemical capacitor [10,11] and tissue engineering [12–14]. These applications are mainly related to the superior properties of PANI such as facile synthesis, environmental stability, tunable conductivity, and biocompatibility [9,12,15]. It is known that the existence of repeated π-bonds within the PANI chains provides the moving of electrons and transferring of counterions (dopants), which are responsible for the conductive nature of polyaniline [4,16]. Many works have been devoted to investigate the effect of various factors such as dopant type [15,17,18], doping level [19–21], solution pH [22–24] and solution temperature [25–27] on the properties of PANI.

It is known that polyaniline has different forms, concerning various oxidation and doping levels [28]. Fig. 1 shows a chemical scheme, outlining the redox behavior of PANI at which the electron and proton transfer occur between the various forms. Leuceomeraldine base (LE) and emeraldine base (EB) are the completely reduced and intermediate

oxidized state, respectively, which have a nonconductive nature. However, EB can be transformed into the conductive state of PANI, called emeraldine salt (ES), by treating EB with an aqueous protonic acid (see Fig. 1) [29].

The approach of some works is to quantitatively analyze the experimental data using the specific relations [30,31]. In this regard, some researchers found that the doping/dedoping process of PANI is under a diffusion-control mechanism [17,30,32,33] and hence, the diffusion coefficient of dopants and the number of transferred electrons were estimated using the well-known Randles-Sevcik equation [30,34]. Some others estimated the electron transfer rate constant based on Laviron's theory [31].

These relations are derived on the basis of two different categories of mathematical modeling: in the first group, it has been assumed that by applying a potential on the electrode, the electroactive species could diffuse from electrolyte bulk towards the electrode surface followed by the redox reactions near the electrode surface; (Randles-Sevcik equation) [35]. In the second group, it has been supposed that the electroactive species are early adsorbed to the electrode surface, and hence the redox reactions occur without the requirement of any diffusion (Laviron's theory) [36,37].

Moreover, various activities have been performed to model the electrochemical behavior of conductive polymers and especially polyaniline. Some researchers have developed a thermodynamic model to describe the redox switching of electroactive polymers

* Corresponding author at: Chemical Engineering Department, Faculty of Engineering, Ferdowsi University of Mashhad, Mashhad, Iran.
  E-mail address: arefinia@um.ac.ir (R. Arefinia).

Leuceomeraldine base (LB)

-2e   +2e
-2H$^+$ +2H$^+$

Emeraldine base (EB)

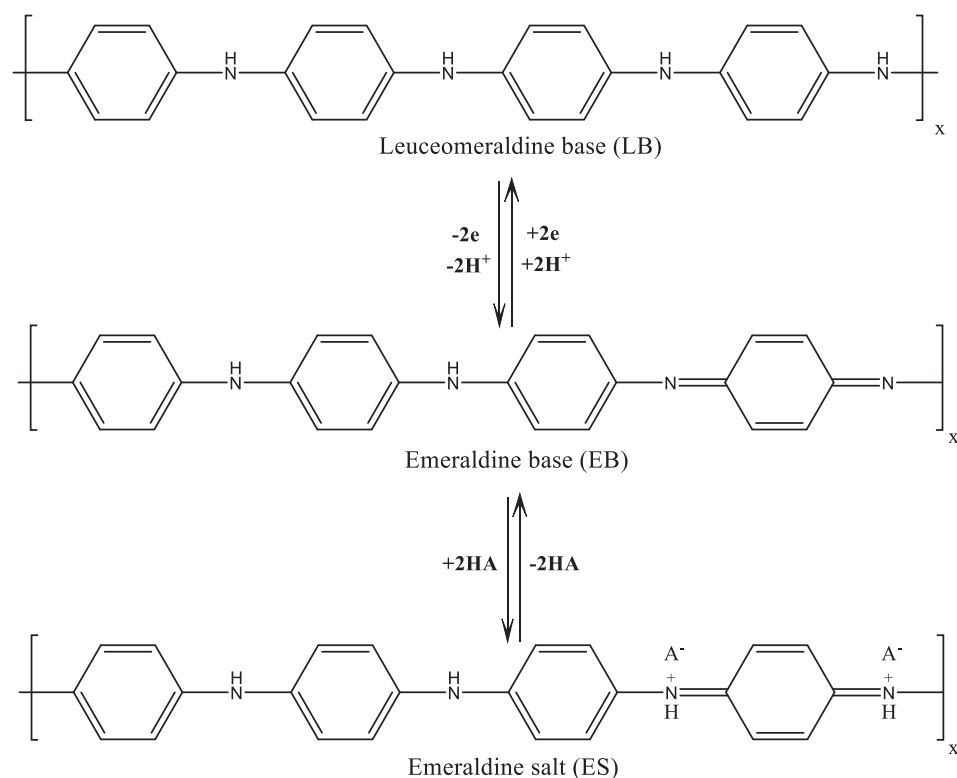+2HA   -2HA

Emeraldine salt (ES)

Fig. 1. Schematic of different forms of PANI.

[38–41]. Briefly, they consider that the redox and doping/dedoping processes take place in one stage, and a conformational change in the molecular structure of PANI occurs due to the income or outcome of the water molecule. Albery et al. modeled the charge conduction process in the conductive polymers by proposing a transmission line for the motion of electron and ions, separately [42–44]. Saveant et al. proposed a model for electron transfer between active sites and the movement of associated counterions [45]. According to the best of our knowledge, the physical spatial separation of the electron transfer reaction and the anion doping process has not been considered to model the electrochemical behavior of a conductive film like polyaniline.

The aim of the present work is to propose a new mathematical model to consider the first redox reaction of PANI film associated with a separate doping/dedoping process (LE ↔ ES, according to Fig. 1). The modeling is based on the fast-kinetic electrochemical reaction, and the mass transfer of dopants within the electrolyte follows the Fickian diffusion. Furthermore, this model was mainly applied for a PANI film and was evaluated by a reliable experimental work reported in the literature. After that, the effects of dopant bulk concentration (C_A^*), potential scan rate (v), adsorption rate constant (k_{ad}), and desorption rate constant (k_{de}) on the redox behavior of a PANI film were systematically studied using the proposed mathematical model (PMM). Moreover, the results were well interpreted by the concentration variations of reduced and doped sites at the PANI film surface.

2. Theory

2.1. Mathematical modeling

In this work, the system involves an electrode covered with a thin PANI film subjected to an electrolyte solution containing dopant anions (Fig. 2).

When an oxidizing potential is applied to the electrode, the interaction of PANI film with the electrolyte processed through three sequential steps:

Step 1: In an electrochemical reaction, reduced (Red) sites are converted to oxidized (Ox) sites, corresponded to the transformation of LB to EB, as the following equation [28,46]:

$$\text{Red} \rightleftarrows \text{Ox} + \text{H}^+ + \text{e}^- \tag{1}$$

Step 2: In a diffusion process within the electrolyte, dopant anions (A$^-$) diffuse from the solution bulk towards the PANI film.
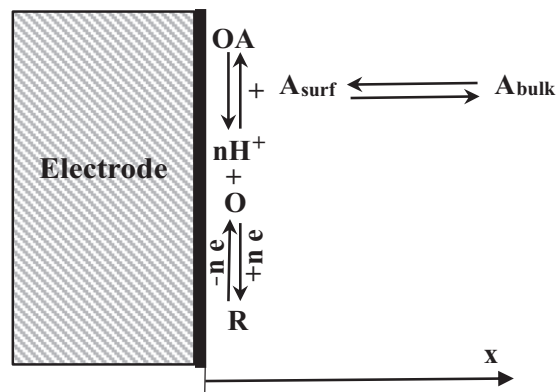
Fig. 2. Schematic of the redox and doping-dedoping processes of a PANI film.

Step 3: In an adsorption process, EB is transformed to ES by the adsorption of the dopant anions (A^-) on the Ox sites, yielding the production of the doped sites (OA) as the following equation:

$$Ox + A^- + H^+ \rightleftarrows OA \tag{2}$$

It is reasonable to state that under applying a reducing potential, the previous steps occur in a reverse direction.

The proposed mathematical model (PMM) has been developed on the basis of the following assumptions:

- The PANI film is thin enough, allowing to consider a compact structure and solid-state, which has been well addressed by Carlin et al. [47]. Therefore, the film porosity is too low that the electrolyte uptake into the film can also be neglected. In this situation, the active sites are placed on the film surface, and the electron transfer together with dopant adsorption occur at the film/solution interface, preventing the formation of an electrical field. In other words, the entry of dopant at the film surface is only controlled by the redox event.
- The electrolyte is stagnant and conductive, so the convection and migration phenomena for dopants are neglected.
- The diffusion process within the electrolyte is unsteady and Fickian, like other studies [42–45,48].
- It was assumed that the adsorption kinetic is independent of electrode potential. This assumption can be concluded from other works [49–51], where they noted that the doping process continues even after switching the potentials in cyclic voltammetry experiments. Additionally, it was assumed that there is no interaction between the adsorbed dopants (Langmuirian adsorption).
- The electrochemical reaction is considered to be fast, so the Nernest equation can be used to relate the redox site concentrations as well addressed before [42–44].

According to these assumptions, the time-dependent equation for the diffusion of dopant anions (A^-) is described using Fick's second law:

$$\frac{\partial C_A}{\partial t} = D_A \frac{\partial^2 C_A}{\partial x^2} \tag{3}$$

where C_A (in mol m^{-3}) and D_A (in m^2 s^{-1}) are the concentration and diffusion coefficient of dopant anions, respectively. At the initial time ($t = 0$), C_A is homogenous throughout the electrolyte and equals the dopant bulk concentration (C_A^*):

$$C_A|_{t=0} = C_A^* \tag{4}$$

The composition of the bulk solution does not change with time, so the first boundary condition is as the following equation:

$$C_A|_{x\to\infty} = C_A^* \tag{5}$$

At the interface of the solution and film surface, the mass flux of dopants equals the rate of dopant adsorption minus the rate of dopant desorption. Therefore, according to the assumptions of conventional diffusion and Langmuirian adsorption, the second boundary condition at the film surface can be written as:

$$-D_A \frac{dC_A}{dx}\Big|_{x=0} = -k_{ad} C_A C_H \Gamma_{Ox} + k_{de} \Gamma_{OA} \tag{6}$$

here, Γ_{Ox} (in mol m^{-2}) and Γ_{OA} (in mol m^{-2}) represent the surface concentration of Ox sites and OA sites (sites occupied by dopant adsorption), respectively. The parameter C_H denotes the hydrogen ion concentration. k_{ad} (in m^6 mol^{-2} s^{-1}) and k_{de} (in s^{-1}) are the adsorption and desorption rate constants, respectively.

Similarly, Eqs. (3) through (5) can be applied for the hydrogen ions as follows:

$$\frac{\partial C_H}{\partial t} = D_H \frac{\partial^2 C_H}{\partial x^2} \tag{7}$$

here, D_H is the diffusion coefficient of hydrogen ions. At the initial time, C_H equals the bulk concentration of hydrogen ions (C_H^*).

$$C_H|_{t=0} = C_H^* \tag{8}$$

The first boundary condition for hydrogen ions is similar to the dopant anions as follows:

$$C_H|_{x\to\infty} = C_H^* \tag{9}$$

At the solution/film interface, the mass flux of hydrogen ions, concerning the redox reaction together with Langmuirian adsorption, is written as:

$$-D_H \frac{dC_H}{dx}\Big|_{x=0} = -k_{ad} C_A C_H \Gamma_{Ox} + k_{de} \Gamma_{OA} - \frac{d\Gamma_{Red}}{dt} \tag{10}$$

To solve the PDE equations, derived for dopant anions and protons, the variables Γ_{Ox} and Γ_{OA} could be determined using the electrochemical and doping processes on the film surface. For this purpose, the relation between concentrations of Red and Ox sites is expressed by the Nernst equation as [28]:

$$E = E^{0'} + \frac{RT}{F} \ln \frac{\Gamma_{Ox} C_H}{\Gamma_{Red}} \tag{11}$$

here, E (in V) is the electrode potential, $E^{0'}$ (in V) the formal potential of PANI redox reaction, R (in J mol^{-1} K^{-1}) gas universal constant, T (in K) absolute temperature and F is Faraday constant. According to Eq. (11), Γ_{Red} (in mol m^{-2}) symbolizes the surface concentration of Red sites in the PANI film and can be obtained from Eq. (11) as:

$$\Gamma_{Red} = \Gamma_{Ox} C_H \exp\left(\frac{nF\left(E - E^{0'}\right)}{RT}\right) \tag{12}$$

It can be reasonable to assume that the total surface concentration of active sites at the PANI film, Γ^* (in mol m^{-2}) is constant and does not change with time as:

$$\Gamma_{Ox} = \Gamma^* - \Gamma_{Red} - \Gamma_{OA} \tag{13}$$

Thus, Γ_{Ox} is obtained by the combination of Eqs. (12) and (13) as follows:

$$\Gamma_{Ox} = (\Gamma^* - \Gamma_{OA}) / \left(1 + C_H \exp\left[\frac{nF\left(E - E^{0'}\right)}{RT}\right]\right) \tag{14}$$

To determine Γ_{OA}, Fig. 2 indicates that the OA sites contribute only to the adsorption reaction. Thus, the net change in Γ_{OA} per time unit is related to the production and consumption rate in the adsorption and desorption reaction, respectively, as the following expression:

$$\frac{d\Gamma_{OA}}{dt} = k_{ad} C_A C_H \Gamma_{Ox} - k_{de} \Gamma_{OA} \tag{15}$$

In this equation, Γ_{Ox} can be substituted from Eq. (14) as follows:

$$\frac{d\Gamma_{OA}}{dt} = k_{ad}C_A \left[\frac{(\Gamma^* - \Gamma_{OA})}{1 + C_H exp\left(\frac{-nF(E - E^{0'})}{RT}\right)} \right] - k_{de}\Gamma_{OA} \qquad (16)$$

All active sites, placed on the surface of PANI film, are initially in the reduced form, and the surface concentrations of Ox and OA sites are equal to zero, so their initial conditions are given as:

$$\Gamma_{Red}|_{t=0} = \Gamma^*, \Gamma_{Ox}|_{t=0} = \Gamma_{OA}|_{t=0} = 0 \qquad (17)$$

To study the redox behavior of electroactive species, cyclic voltammetry is a powerful method [35,36]. Therefore, in this work, the proposed mathematical model (PMM) has been developed based on this electrochemical method; at which the potential is positively scanned, and then at a specified potential known as the switching potential (E_{sw}), the direction of potential sweep is reversed. These can be presented by the following relations:

$$E = \begin{cases} E_i + vt & t \leq t_{sw} \\ E_i + 2vt_{sw} - vt & t \geq t_{sw} \end{cases} \qquad (18)$$

where E_i is the initial potential, t_{sw} is the switching time, and v is the potential scan rate.

The current value (I) of cyclic voltammogram can be calculated by the hypothesis of the net rate of change in Γ_{Red} with time:

$$\frac{I}{nFA} = -\frac{d\Gamma_{Red}}{dt} \qquad (19)$$

here, A is the surface area of the PANI film (in m^2) and n the number of exchanged electrons.

Briefly, it can be stated that the PMM constitutes a set of equations: an ordinary differential equation and two partial differential equations associated with the appropriate boundary and initial condition equations. These equations were solved according to the finite element method in COMSOL Multiphysics software. The PMM was run on a personal computer with a 4×2.7 GHz and an 8 GB of memory. Additionally, the size of the domain grid was 4×10^{-5} and the domain was meshed denser near the film surface. Note that the accuracy of the domain grid was checked by the fact that the similar results were obtained for the ones involving higher number of grid points. In detailed, the time step was changed from 0.1 to 0.001 s and the PMM was run until the concentration of each species was within the difference of 1% (convergence error <1%).

2.2. Parametric study

The effect of various parameters including the adsorption and desorption rate constants (k_{ad} and k_{de}), the bulk concentration of dopant anions (C_A^*), and the potential sweep rate (v) on the electrochemical behavior of a PANI film were parametrically studied using the mathematical model developed in the present work.

To conduct a systematic parametric analysis using the PMM; first, a reference system with specific conditions was defined. Then, the value of each parameter in the proposed mathematical model (PMM) was separately changed in a specific range while the others were kept constant relative to the reference system. The reference system and the variation ranges were selected on the basis of the work of MacDiarmid and Epstein [28] (in Table 1). This work was also applied to evaluate the PMM in the following section.

Table 1
The parameters chosen for the reference system and their variations to study the electrochemical response of PANI film using PMM.

Parameter	Symbol (unit)	Basic value	Variations
Adsorption rate constant	k_{ad} (L^2 mol^{-2} s^{-1})	50	10, 50, 100
Desorption rate constant	k_{de} (s^{-1})	0.4	0.5, 1, 1.5
Bulk concentration of dopant	C_A^* (mol L^{-1})	1	1, 3, 6
Potential scan rate	v (mV s^{-1})	50	10, 50, 100

In this regard, the value of temperature (T) and the number of exchanged electrons (n) was considered to be equal to 298 K and 1 [34], respectively. The values of the diffusion coefficient of anion and hydrogen ion were assumed to be equal 1×10^{-9} and 9×10^{-9} m^2 s^{-1}, respectively [52]. The value of redox formal potential ($E^{0'}$) was selected 0.1 V and the potential was swept around the selected $E^{0'}$ between −0.1 and 0.4 V according to the work of MacDiarmid and Epstein [28]. The parameters k_{ad}, k_{de}, and Γ^* are three adjustable parameters that can be individually estimated by fitting the experimental data to the PMM.

3. Results and discussion

3.1. Evaluation of the proposed mathematical model (PMM)

Some known studies about the electrochemical behavior of conductive polymers especially in the case of PANI was performed by MacDiarmid, who received the chemistry Nobel prize for his efforts in 2000. According to one of these works [28], for PANI at pH ≤ 0, the electrochemical reaction is one electron/one proton fast kinetic reaction according to the linearity relation together with the slope of 59 mV per pH unit for the plot of E_p vs. pH. This electrochemical reaction agrees with that assumed in the present work. With respect to this work [28], the potential scan rate (v) was 50 mV s^{-1}, HCl concentration was 1 mol L^{-1}, and the electrode surface area was 1 cm^2.

In these conditions, the PMM was evaluated using the experimental data reported by MacDiarmid [28] (see Fig. 3). It is apparent that the shape of curves resulted from the PMM and experimental data, is generally similar; additionally, there is a good consistency from the aspect of intensity and position of the oxidation peak. In this context, the value of
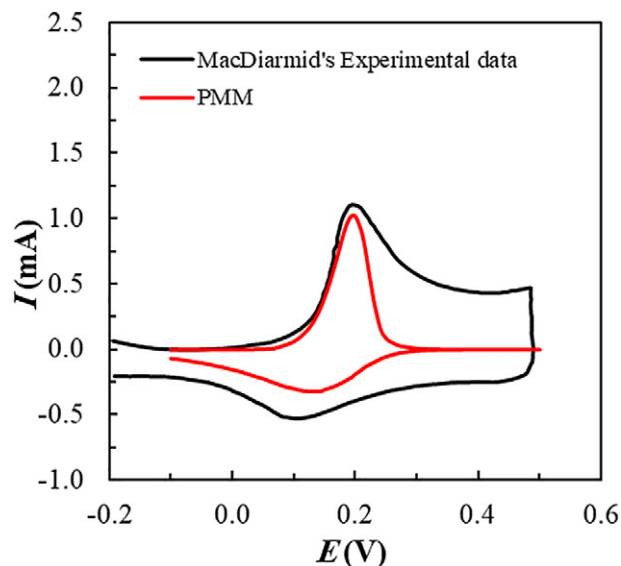

Fig. 3. Evaluation of PMM using the experimental data reported by MacDiarmid and Epstein [28].

parameters Γ^*, $E^{0'}$, k_{ad} and k_{de} were estimated and are equal to 1.6 $\times 10^{-4}$ mol m^{-2}, 0.1 V, 50 L^2 mol^{-2} s^{-1} and 0.4 s^{-1}, respectively. However, the difference appeared after the oxidation peak may be because of both the capacitive current and the effect of second redox reaction which is out of scope of the present work.

3.2. Effect of dopant bulk concentration

Dopant bulk concentration (C_A^*) directly affects the rate of the doping process according to Eq. (15), and hence on the redox reaction of polyaniline film. Therefore, the effect of C_A^*, varying between 1 and 3 mol L^{-1} at the constant pH was studied using PMM, and the obtained voltammograms are shown in Fig. 4.

It is evident that the shape of oxidation peaks is sharp, but it is broad for the reduction peaks which agrees with some experimental works [28,46,53,54]. Moreover, for each voltammogram, the oxidation and reduction peaks appear at different potentials, in contrast with that reported for the behavior of electroactive species, adsorbed on the electrode surface with a fast kinetic redox reaction, [36,37] which will be discussed later. Fig. 4 shows that the increase of C_A^* from 1 to 3 mol L^{-1} is associated with a slight increase of oxidation peak current and the shift of redox peak couple to the lower potentials. In this regard, Liu et al. [54] observed similar behavior for the shift of redox peak potential with a decrease in the number of PANI nanotube layers on the electrode which can be attributed to the reduction in the concentration of active sites (Γ^*) according to the concepts of the present work. In other words, the effect of increase in C_A^* relative to Γ^* on the electrochemical reaction is as equal as the effect of decrease in Γ^* relative to C_A^*.

To better interpret the observed electrochemical behaviors, variations of concentration for different film sites, including Γ_{Red}, Γ_{OA}, and Γ_{Ox}, were studied using PMM and the obtained results for Γ_{Red} and Γ_{OA} are shown in Fig. 5. Note that the concentration of Ox sites (Γ_{Ox}) is negligible in comparison with Γ_{Red} and Γ_{OA}, thereby, the relevant diagram has not been represented. According to Fig. 5, for the oxidation half cycle (OHC), registered between −0.1 and 0.4 V, the value of Γ_{Red} decreases, and Γ_{OA} increases significantly as a result of the consumption of Red sites and the production of OA sites, respectively. In the case of reduction half cycle (RHC), registered from 0.4 to −0.1 V, a reverse trend of variation for both Γ_{Red} and Γ_{OA} is observed according to the following equation:

$$\text{Red} \rightleftarrows \text{Ox} \rightleftarrows \text{OA} \tag{20}$$

Regarding this equation, the negligible value of Γ_{Ox} can be explained by the fast rate of doping process and electrochemical reaction for OHC and RHC, respectively. It can be found from Eq. (20) that the reduction
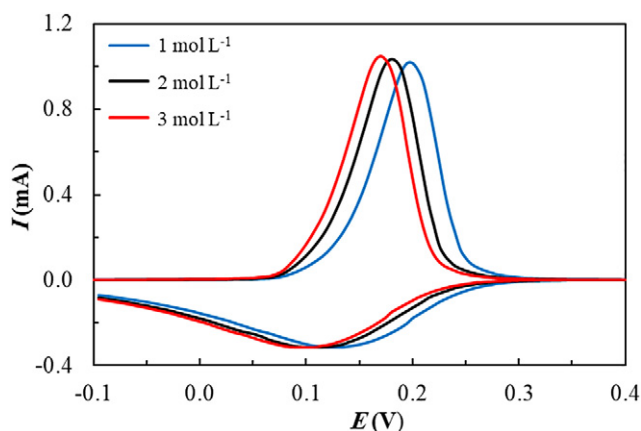
Fig. 5. Effect of bulk concentration of dopant (C_A^*) at the constant pH on the variation of a) Γ_{Red}, and b) Γ_{OA} obtained using PMM at the conditions presented in Table 1.

reaction (Red ← Ox) depends upon the rate of desorption of dopants, suggesting a lower rate of reduction compared to the oxidation rate and can be considered as the main reason for the broad shape of reduction peaks (in Fig. 4).

Furthermore, Fig. 5 shows that the increment of C_A^* causes the enhancement in both the consumption of Red sites and the production of OA sites in OHC. This indicates that the doping process accelerates the electrochemical reaction and hence the higher conversion rate of Red sites to Ox sites according to Eq. (20). Therefore, the doping process provides the increase of oxidation peak current and the shift of potential to the lower values as observed by the voltammograms (Fig. 4).

For the RHC, since the reduction reaction (Red ← Ox) depends on the dedoping process and hence the higher amounts of dopant ions reduces the production rate of Ox sites (Ox ← OA), thereby, a higher potential driving force is required to start the reduction reaction. This causes to shift the reduction peak potential to the lower values.

3.3. Effect of potential scan rate

Potential scan rate (v) determines the time frame of the redox reaction and hence the lower sweep rate of potential, the higher time of reaction. Therefore, parameter v was varied between 10 and 100 mV s^{-1}, chosen according to the experimental works [17,28,46] and the obtained voltammograms are shown in Fig. 6.

Fig. 4. Effect of bulk concentration of dopant (C_A^*) at the constant pH on the cyclic voltammetry diagrams obtained using PMM at the conditions presented in Table 1.
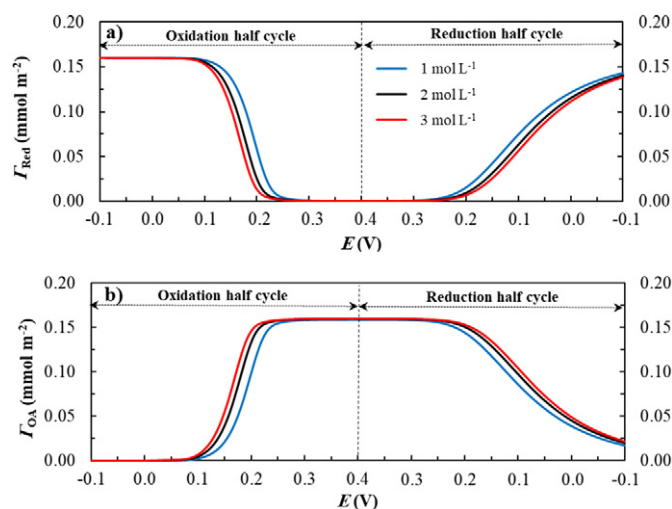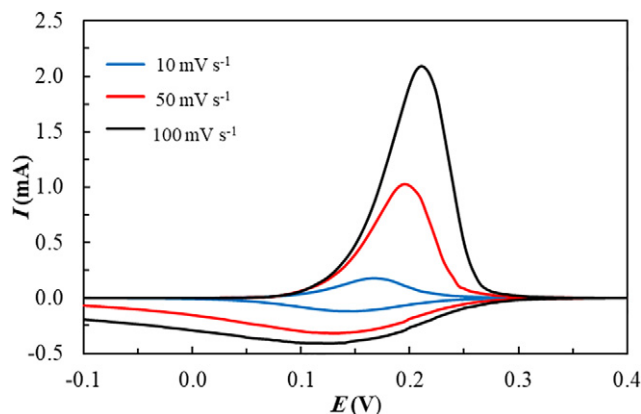
Fig. 6. Effect of potential scan rate (v) on the cyclic voltammetry diagrams obtained using PMM at the conditions presented in Table 1.

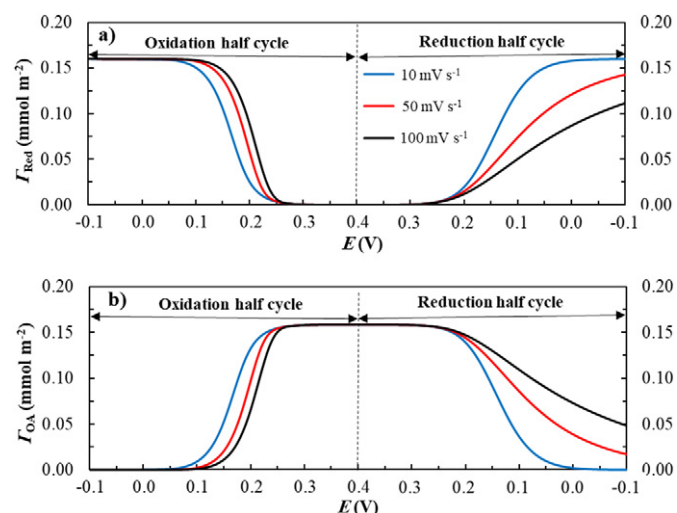Fig. 7. Effect of potential scan rate (v) on the variations of a) Γ_{Red}, and b) Γ_{OA} obtained using PMM at the conditions presented in Table 1.

Fig. 8. Effect of adsorption rate constant (k_{ad}) on the cyclic voltammetry diagrams obtained using PMM at the conditions presented in Table 1.

The decrease of v from 100 to 10 mV s^{-1} results in the decrement of both oxidation and reduction peaks, while the separation in peak potential is lowered where a similar trend of variations as a function of v was addressed previously [17,46]. To better explain the effect of potential scan rate on the cyclic voltammograms, variations of Γ_{Red}, Γ_{OA} versus v are shown in Fig. 7.

When parameter v decreases from 100 to 10 mV s^{-1}, the time required to complete the cycle and hence, the time of redox reaction increases. This causes a decrease in the rate of consumption and production of red sites for the OHC and RHC, respectively. At the same time, a reverse behavior can be identified for the OA sites. Therefore, it is reasonable to state that a decrease in the rate of both forward and backward electrochemical reactions, regarding Eqs. (1) and (19) is responsible for the reduction in the peak current versus scan rate as observed in Fig. 6.

Moreover, an increase in the time of reaction with a decrease of v is associated with the shift of oxidation peak to the lower potentials (Fig. 6), which can be due to the higher amounts of doping, affecting the electrochemical reaction according to Eq. (20). This behavior is like that obtained by the increase in the dopant concentration and was well discussed in the previous section.

For the RHC, the enhancement of reaction time provides the higher amounts of Ox sites with the dedoping process (Fig. 7 b); therefore, a lower potential driving force is required to start the reduction reaction, so the reduction peak moves to the higher potentials (see Fig. 6).

3.4. Effect of adsorption rate constant (k_{ad})

The parameter k_{ad} affects directly on the rate of doping process according to Eq. (15). The effect of k_{ad}, varying between 10 and 100 L^2 mol^{-2} s^{-1} was evaluated using PMM, and the obtained voltammograms are shown in Fig. 8. It can be found that the increase of k_{ad} from 10 to 100 L^2 mol^{-2} s^{-1} has a nearly similar effect on both the oxidation and reduction peak potentials, i.e. they shift markedly to the lower potentials. Furthermore, the oxidation peak current increases slightly, but no significant change in the reduction current peak can be observed. This implies that the effect of k_{ad} on the OHC is higher than that for the RHC.

The effect of k_{ad} on the variations of Γ_{Red}, Γ_{OA} were studied using PMM, and the obtained results are shown in Fig. 9. It is apparent that when k_{ad} increases from 10 to 100 L^2 mol^{-2} s^{-1}, the consumption of
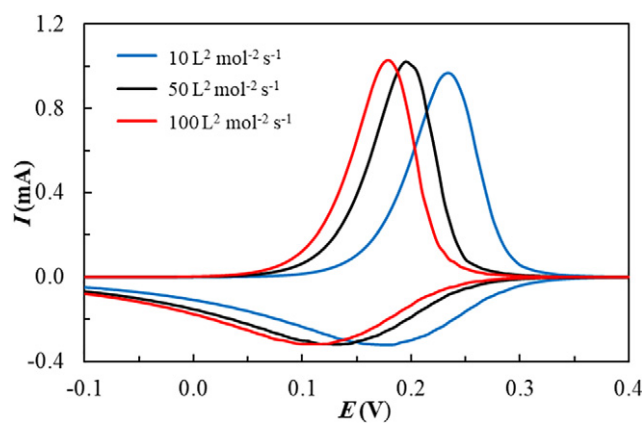
Red sites and the production of OA sites for the OHC start from the lower potentials due to the effect of doping process as discussed before. These can be considered as the reasons for the increase of oxidation peak current and the shift of oxidation peak to the lower potentials (Fig. 8).

In the RHC, when k_{ad} increases, the production of Red sites and consumption of OA sites initiate from the lower potentials (see Fig. 9), because a higher potential driving force is required to start the reduction reaction like to that reported for the effect of C_A^*. This driving force explains why the reduction peak shifts to the lower potentials (Fig. 8).

3.5. Effect of desorption rate constant (k_{de})

The effect of desorption rate constant (k_{de}) is important as well as k_{ad} on the doping rate according to Eq. (15). In this regard, the effects of different values of k_{de}, including 0.5, 1.0 and 1.5 s^{-1} (given in Table 1) on the CV curves were studied using the PMM, and the obtained data are displayed in Fig. 10. As seen, the variation of k_{de} has a significant effect on the RHC compared with OHC. This behavior is generally inverse to that observed for the effect of k_{ad} on the cyclic voltammograms (Fig. 8). However, a precise comparison between Figs. 8 and 10 reveals
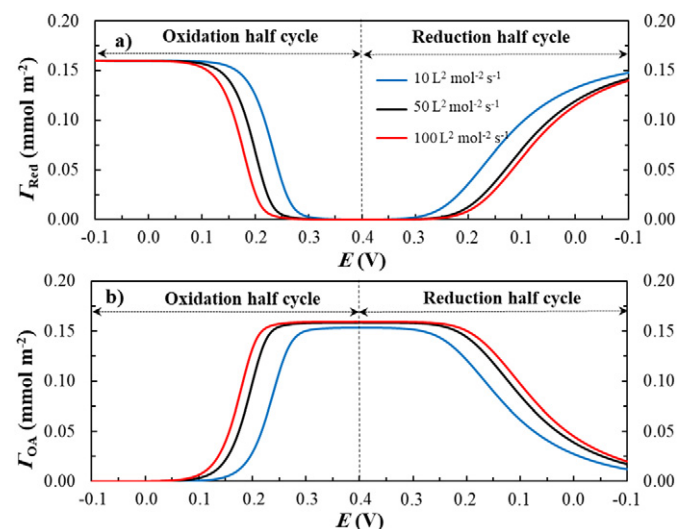

Fig. 9. Effect of adsorption rate constant (k_{ad}) on the variations of a) Γ_{Red}, and b) Γ_{OA} obtained using PMM at the conditions presented in Table 1.
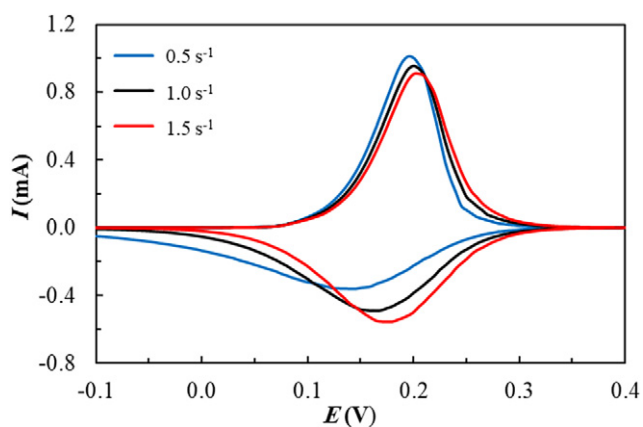
Fig. 10. Effect of desorption rate constant (k_{de}) on the cyclic voltammetry diagrams obtained using PMM at the conditions presented in Table 1.

that the effect of k_{de} on the reduction peak current is higher than the effect of k_{ad} on the oxidation peak current, which prevents applying an equilibrium constant (k_{ad}/k_{de}) to study the electrochemical behavior of the PANI film by the cyclic voltammograms.

Fig. 11 shows the variations of Γ_{Red} and Γ_{OA} with k_{de}. It is apparent that for the RHC, when k_{de} increases from 0.5 to 1.5 s^{-1}, Γ_{Red} and Γ_{OA} reach their maximum and minimum values, respectively, at the higher potentials. This behavior can be directly related to the effect of dedoping process on the reduction reaction; indeed, the higher rate of dedoping facilitates the reduction reaction, which could be considered as the main reason for the shift of reduction peak to the higher potentials and the increase of peak current (Fig. 10). Moreover, this explains why the reduction peak current was increased with the oxidant (nitrite) concentration for the PANI nanotube coated on an electrode surface reported previously [53] where the increase of nitrite concentration causes the increase of dedoping process as a result of enhancement in the concentration of ES.

On the other hand, Fig. 11 indicates that the variation of k_{de} has a negligible effect on the peak current and potential in the OHC, which is in good agreement with those observed by the voltammograms (Fig. 10).
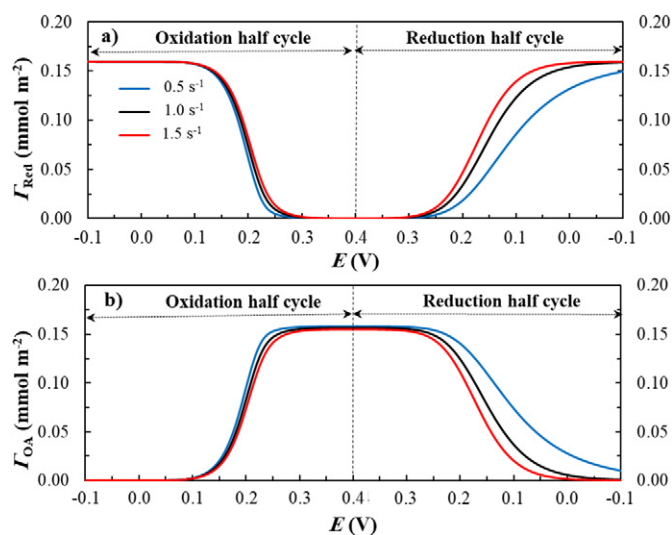

Fig. 11. Effect of desorption rate constant (k_{de}) on the variations of a) Γ_{Red}, and b) Γ_{OA} obtained using PMM at the conditions presented in Table 1.

4. Conclusion

In this work, a one-dimensional mathematical model was proposed to deal with the electrochemical behavior of a thin PANI film during the redox and doping/dedoping process using the cyclic voltammetry method. The effect of different parameters including C_A^*, v, k_{ad} and k_{de} on the redox and doping-dedoping process of a thin PANI film was systematically studied using CV curves together with the variations of Γ_{Red} and Γ_{OA}.

The cyclic voltammograms showed the sharp shape of the oxidation peak compared to the broad shape for the reduction peak, and the existence of a separation between the oxidation and reduction peak potentials. Concerning the variations of Γ_{Red} and Γ_{OA}, these observations could be directly attributed to the influence of doping/doping process on the redox reaction.

The parametric study by PMM revealed that the increase of parameters k_{ad} and C_A^* causes the shift of voltammograms to the lower potentials due to increasing the rate of doping process. The decrease of v resulted a reduction in the currents of redox peak couple because of the increment in the rate of redox reaction. At the same time, the enhancement of reaction time causes the increase of both the doping and dedoping process for the oxidation and reduction half cycle (OHC and RHC), respectively. This results in a decrease of redox peaks separation. The increment of k_{de} is associated with the increase of reduction peak current and the shift of this peak to the higher potentials which is related to the increase in the effect of dedoping process on the reduction reaction. Generally, it can be stated that k_{ad} and k_{de} had the main effect on OHC and RHC, respectively.

It can be concluded that the PMM provided a valuable tool to study and compare the effect of different parameters on the electrochemical behavior of a PANI film based on the assumptions of the present work.

Author contribution statement

Fatemeh Ziaei Moghaddam: Conceptualization, Methodology, Software, Visualization, Writing- Original draft preparation.

Reza Arefinia: Supervision, Methodology, Conceptualization, Writing - Reviewing and Editing.

Declaration of competing interest

The authors declare that they have no known competing financial interests or personal relationships that could have appeared to influence the work reported in this paper.

References

[1] E. Genies, A. Boyle, M. Lapkowski, C. Tsintavis, Polyaniline: a historical survey, Synth. Met. 36 (1990) 139–182.
[2] H. Nazari, R. Arefinia, Electrochemical and quantum chemical study of polyaniline nanoparticles suspension in HCl and H2SO4, Electrochim. Acta 320 (2019), 134553.
[3] P.C. Ramamurthy, A.N. Mallya, A. Joseph, W.R. Harrell, R.V. Gregory, Synthesis and characterization of high molecular weight polyaniline for organic electronic applications, Polym. Eng. Sci. 52 (2012) 1821–1830.
[4] H. Shirakawa, A. McDiarmid, A. Heeger, Twenty-five years of conducting polymers, Chem. Commun. (2003) (2003) 1–4.
[5] Y. Gao, J.A. Syed, H. Lu, X. Meng, Anti-corrosive performance of electropolymerized phosphomolybdic acid doped PANI coating on 304SS, Appl. Surf. Sci. 360 (2016) 389–397.
[6] R. Arefinia, A. Shojaei, H. Shariatpanahi, J. Neshati, Anticorrosion properties of smart coating based on polyaniline nanoparticles/epoxy-ester system, Prog. Org. Coat. 75 (2012) 502–508.
[7] W. Chu, Q. Zhou, S. Li, W. Zhao, N. Li, J. Zheng, Oxidation and sensing of ascorbic acid and dopamine on self-assembled gold nanoparticles incorporated within polyaniline film, Appl. Surf. Sci. 353 (2015) 425–432.
[8] X. Zhang, B. Ogorevc, J. Wang, Solid-state pH nanoelectrode based on polyaniline thin film electrodeposited onto ion-beam etched carbon fiber, Anal. Chim. Acta 452 (2002) 1–10.
[9] I. Fratoddi, I. Venditti, C. Cametti, M.V. Russo, Chemiresistive polyaniline-based gas sensors: a mini review, Sensors Actuators B Chem. 220 (2015) 534–548.
[10] G. Otrokhov, D. Pankratov, G. Shumakovich, M. Khlupova, Y. Zeifman, I. Vasil'eva, O. Morozova, A. Yaropolov, Enzymatic synthesis of polyaniline/multi-walled carbon

nanotube composite with core shell structure and its electrochemical characterization for supercapacitor application, Electrochim. Acta 123 (2014) 151–157.

[11] C. Wang, L. Sun, Y. Zhou, P. Wan, X. Zhang, J. Qiu, P/N co-doped microporous carbons from H3PO4-doped polyaniline by in situ activation for supercapacitors, Carbon 59 (2013) 537–546.

[12] T.H. Qazi, R. Rai, A.R. Boccaccini, Tissue engineering of electrically responsive tissues using polyaniline based polymers: a review, Biomaterials 35 (2014) 9068–9086.

[13] P.R. Bidez, S. Li, A.G. MacDiarmid, E.C. Venancio, Y. Wei, P.I. Lelkes, Polyaniline, an electroactive polymer, supports adhesion and proliferation of cardiac myoblasts, J. Biomat. Sci-Polym. E. 17 (2006) 199–212.

[14] H.j. Wang, L.w. Ji, D.f. Li, J.Y. Wang, Characterization of nanostructure and cell compatibility of polyaniline films with different dopant acids, J. Phys. Chem. B 112 (2008) 2671–2677.

[15] Q. Hao, W. Lei, X. Xia, Z. Yan, X. Yang, L. Lu, X. Wang, Exchange of counter anions in electropolymerized polyaniline films, Electrochim. Acta 55 (2010) 632–640.

[16] T.H. Le, Y. Kim, H. Yoon, Electrical and electrochemical properties of conducting polymers, Polymers 9 (2017) 150–182.

[17] M. Gao, Y. Yang, M. Diao, S.g. Wang, X.h. Wang, G. Zhang, G. Zhang, Exceptional ion-exchange selectivity for perchlorate based on polyaniline films, Electrochim. Acta 56 (2011) 7644–7650.

[18] T.M. Wu, Y.W. Lin, Synthesis and characterization of hollow polyaniline microtubes and microbelts with nanostructured walls in sodium dodecyl sulfate micellar solutions, Polym. Eng. Sci. 48 (2008) 823–828.

[19] J.K. Avlyanov, Y. Min, A.G. MacDiarmid, A.J. Epstein, Polyaniline: conformational changes induced in solution by variation of solvent and doping level, Synth. Met. 72 (1995) 65–71.

[20] P. Kiattibutr, L. Tarachiwin, L. Ruangchuay, A. Sirivat, J. Schwank, Electrical conductivity responses of polyaniline films to SO2–N2 mixtures: effect of dopant type and doping level, React. Funct. Polym. 53 (2002) 29–37.

[21] H. Nazari, R. Arefinia, An investigation into the relationship between the electrical conductivity and particle size of polyaniline in nano scale, Int. J. Polym. Anal. Ch. 24 (2019) 178–190.

[22] J.C. Chiang, A.G. MacDiarmid, 'Polyaniline': protonic acid doping of the emeraldine form to the metallic regime, Synth. Met. 13 (1986) 193–205.

[23] W.W. Focke, G.E. Wnek, Y. Wei, Influence of oxidation state, pH, and counterion on the conductivity of polyaniline, J. Phys. Chem. 91 (1987) 5813–5818.

[24] X.Y. Peng, F. Luan, X.X. Liu, D. Diamond, K.T. Lau, pH-controlled morphological structure of polyaniline during electrochemical deposition, Electrochim. Acta 54 (2009) 6172–6177.

[25] L.H. Romarís, M.J. Abad, M.V. González Rodríguez, A. Lasagabáster, P. Costa, S. Lanceros Méndez, Cyclic temperature dependence of electrical conductivity in polyanilines as a function of the dopant and synthesis method, Mater. Design. 114 (2017) 288–296.

[26] J. Stejskal, A. Riede, D. Hlavatá, J. Prokeš, M. Helmstedt, P. Holler, The effect of polymerization temperature on molecular weight, crystallinity, and electrical conductivity of polyaniline, Synth. Met. 96 (1998) 55–61.

[27] K.M. Molapo, P.M. Ndangili, R.F. Ajayi, G. Mbambisa, S.M. Mailu, N. Njomo, M. Masikini, P. Baker, E.I. Iwuoha, Electronics of conjugated polymers (I): polyaniline, Int. J. Electrochem. Sci. 7 (2012) 11859–11875.

[28] A.G. MacDiarmid, A.J. Epstein, Polyanilines: a novel class of conducting polymers, Faraday Discuss. Chem. Soc. 88 (1989) 317–332.

[29] A.G. MacDiarmid, "Synthetic metals": a novel role for organic polymers (Nobel lecture), Angew. Chem. Int. Ed. 40 (2001) 2581–2590.

[30] D. Ge, L. Yang, Z. Tong, Y. Ding, W. Xin, J. Zhao, Y. Li, Ion diffusion and optical switching performance of 3D ordered nanostructured polyaniline films for advanced electrochemical/electrochromic devices, Electrochim. Acta 104 (2013) 191–197.

[31] H.W. Park, T. Kim, J. Huh, M. Kang, J.E. Lee, H. Yoon, Anisotropic growth control of polyaniline nanostructures and their morphology-dependent electrochemical characteristics, ACS Nano 6 (2012) 7624–7633.

[32] S. Xiong, Z. Li, M. Gong, X. Wang, J. Fu, Y. Shi, B. Wu, J. Chu, Covalently bonded polyaniline and Para-phenylenediamine functionalized graphene oxide: how the conductive two-dimensional nanostructure influences the electrochromic behaviors of polyaniline, Electrochim. Acta 138 (2014) 101–108.

[33] H. Nazari, R. Arefinia, Electrochemical behavior of polyaniline nanoparticles suspension: adsorption and diffusion, J. Mol. Liq. 288 (2019), 110999.

[34] K. Aoki, J. Chen, Q. Ke, S.P. Armes, D.P. Randall, Redox reactions of polyaniline-coated latex suspensions, Langmuir 19 (2003) 5511–5516.

[35] R.S. Nicholson, I. Shain, Theory of stationary electrode polarography. Single scan and cyclic methods applied to reversible, irreversible, and kinetic systems, Anal. Chem. 36 (1964) 706–723.

[36] E. Laviron, General expression of the linear potential sweep voltammogram in the case of diffusionless electrochemical systems, J. Electroanal. Chem. Interfacial Electrochem. 101 (1979) 19–28.

[37] S. Srinivasan, E. Gileadi, The potential-sweep method: a theoretical analysis, Electrochim. Acta 11 (1966) 321–335.

[38] L. Lizarraga, E.M. Andrade, M.I. Florit, F.V. Molina, Quasi-equilibrium volume changes of polyaniline films upon redox switching. Formal potential distribution and configurational modeling, J. Phys. Chem. B 109 (2005) 18815–18821.

[39] L. Lizarraga, E.M. Andrade, F.V. Molina, Swelling and volume changes of polyaniline upon redox switching, J. Electroanal. Chem. 561 (2004) 127–135.

[40] T.F. Otero, Structural and conformational chemistry from electrochemical molecular machines. Replicating biological functions. A review, Chem. Rec. 18 (2018) 788–806.

[41] D. Posadas, M.I. Florit, The redox switching of electroactive polymers, J. Phys. Chem. B 108 (2004) 15470–15476.

[42] W.J. Albery, C.M. Elliott, A.R. Mount, A transmission line model for modified electrodes and thin layer cells, J. Electroanal. Chem. Interfacial Electrochem. 288 (1990) 15–34.

[43] W.J. Albery, A.R. Mount, A further development of the use of transmission lines to describe the movement of charge in conducting polymers, J. Electroanal. Chem. 388 (1995) 1–9.

[44] W.J. Albery, A.R. Mount, A second transmission line model for conducting polymers, J. Electroanal. Chem. Interfacial Electrochem. 305 (1991) 3–18.

[45] J. Saveant, Electron hopping between fixed sites: equivalent diffusion and migration laws, J. Electroanal. Chem. Interfacial Electrochem. 201 (1986) 211–213.

[46] J.C. LaCroix, A. Diaz, Electrooxidation of Aromatics to Polymer Films, 8, Wiley Online Library, 1987 17–37.

[47] C.M. Carlin, L.J. Kepley, A.J. Bard, Polymer films on electrodes XVI. In situ ellipsometric measurements of polybipyrazine, polyaniline, and polyvinylferrocene films, J. Electrochem. Soc. 132 (1985) 353–359.

[48] F.C. Anson, J.M. Saveant, K. Shigehara, Self-exchange reactions at redox polymer electrodes. A kinetic model and theory for stationary voltammetric techniques, J. Phys. Chem. 87 (1983) 214–219.

[49] M. Kalaji, L. Nyholm, L. Peter, A microelectrode study of the influence of pH and solution composition on the electrochemical behaviour of polyaniline films, J. Electroanal. Chem. 313 (1991) 271–289.

[50] G. Horanyi, G. Inzelt, Anion-involvement in electrochemical transformations of polyaniline. A radiotracer study, Electrochim. Acta 33 (1988) 947–952.

[51] D. Orata, D.A. Buttry, Determination of ion populations and solvent content as functions of redox state and pH in polyaniline, J. Am. Chem. Soc. 109 (1987) 3574–3581.

[52] J. Wang, Analytical Electrochemistry, John Wiley & Sons, 2006.

[53] J. Liu, X. Li, C. Batchelor-McAuley, G. Zhu, R.G. Compton, Nitrite-enhanced charge transfer to and from single polyaniline nanotubes, Chem-Eur. J. 23 (2017) 17823–17828.

[54] J. Liu, G. Zhu, X. Li, C. Batchelor-McAuley, S.V. Sokolov, R.G. Compton, Quantifying charge transfer to nanostructures: polyaniline nanotubes, Appl. Mater. Today 7 (2017) 239–245.